Design and Analysis of Permanent Magnet Linear Synchronous Motor with Special Pole Shape

Xudong Wang
School of Electrical Engineering & Automation, Henan Polytechnic University, Jiaozuo 454000, China
Email: wangxd@hpu.edu.cn

Kai Cao, Haichao Feng, Lili Guo, Xiaozhuo Xu
School of Electrical Engineering & Automation, Henan Polytechnic University, Jiaozuo 454000, China
Email:caokai.pds@gmail.com

Abstract—**Permanent magnet linear synchronous motors (PMLSMs), which have great advantages, such as simple structure, high positioning accuracy, good performance, high thrust force density, high dynamic response, are widely used in high precision direct drive field. As a research focus and difficulty, the force ripper and dynamic characteristic of PMLSM is important for its performance. In this paper, the present research status and characteristics of PMLSM is discussed firstly. Then a 16-pole 15-slot PMLSM is built used finite element method (FEM). Based on the finite element model, the thrust force ripple and minimization technologies, the power factor and efficiency of PMLSM with different load, were solved and analyzed, and an optimized model was got. The analysis result of thrust and magnetic flux density shows that through the new geometry of primary tooth shape, named optimized model, can improve the average thrust and reduce thrust fluctuations. The optimized model also has higher the power factor and efficiency. The back EMF of original and optimized model are also compared and discussed.**

Index Terms—**FEM, PMLSM, thrust ripple, magnetic flux density, back EMF constant, power factor, efficiency**

Ⅰ. INTRODUCTION

Permanent magnet linear synchronous motors (PMLSMs) have great advantages in high precision direct drive field. In recent years, PMLSM has been used in the machine tool, semiconductors and electronics manufacturing, optical instrument and industry automation field. It has many advantages such as simple structure, high positioning accuracy, good dynamic performance, high energy index, fast reaction rate, high sensitivity, good motion following ability, big force density and good controllability. Ref. [1] introduces the principle and present research situation of permanent magnet linear synchronous motor.

There are many researchers and scientists around the world have been engaged in much research aiming at decreasing thrust and speed ripple in order to improving positioning accuracy and dynamic performance of motor. Ref. [2] proposed that the thrust fluctuation can be reduced by proper selection of magnetizing methods and magnet position and shapes. Ref. [3] proposed that the slot effect could be greatly reduced by using fraction slot structure and the thrust ripple was key factor which affected the properties of permanent magnet linear synchronous motors. Ref. [4, 5] proposed that the electro-magnetic field model was built up and analyzed quantificational. And the stator teeth notching can reduce the cogging torque effectively. Ref. [6, 7] summarized the methods of detent force reduction. The optimization of primary structure is one of the methods. Generally speaking, a good motor structure and an excellent control method could restrain the thrust ripple.

In this paper, in order to improve the performance of motor, a novel primary structure for a long-primary 16-pole 15-slot PMLSM has been proposed to reduce the thrust ripple. The performances of PMLSM with the optimized and the original primary structures have been confirmed by the two dimensional (2D) finite element analyses (FEA), respectively. The power factor and efficiency of the optimized model was analyzed and compared with the original model. The back EMF constant was calculated in the final section of paper.

Ⅱ. PRINCIPLE OF FINITE ELEMENT METHOD

Based on variation principle, Clough puts the Finite Element Method in his book in 1960. It has a better application in a lot of project fields in recent years. Especially in electrical engineering area, FEM plays an important role in quantitative analysis and optimization.

All the electromagnetic phenomena can be described by maxwell equations in PMLSM. Generally, the effect of displacement current doesn't be considered, so the air-

Manuscript received October 10, 2011; revised November 10, 2011; accepted November 12, 2011.

National Natural Science Foundation of China (NO. 61074095), Henan Outstanding Person Plan (NO. 104200510021), and Ministry of Education Scientific Research Foundation for Chinese Overseas Returnees and Ministry of Education Research Fund for Doctoral Program of Higher Education, and Henan Province Key Project (NO. 092102210359).

Xudong Wang, Prof., PH.D, doctoral supervisor, research direction on linear motor and modern drive technology.

doi:10.4304/jcp.8.2.478-484

gap magnetic field is stable in vertical direction. The expression of parallel plane field as follows:

$$\begin{cases} rot\vec{H} = \vec{J} \\ div\vec{B} = 0 \\ \vec{B} = \mu_r \mu_0 \vec{H} \end{cases} \quad (1)$$

where $\vec{H}$ is the magnetic field intensity, $\vec{B}$ is the magnetic induction, $\vec{J}$ is current intensity, μ_r is the differential permeability, μ_0 is the permeability of vacuum**.**

Considering the saturation effect of ferromagnetic material, the above vector equation can be simplified as follow:

$$\frac{\partial}{\partial x}\left(\frac{1}{\mu_r \mu_0}\frac{\partial A_z}{\partial x}\right)+\frac{\partial}{\partial y}\left(\frac{1}{\mu_r \mu_0}\frac{\partial A_z}{\partial y}\right) = -\vec{J}_z \quad (2)$$

There is no initial conditions in magnetic field of PMLSM, the solution of field is determined by boundary conditions.

$$\begin{cases} S1: A = A_0 \\ S2: \dfrac{1}{\mu_r \mu_0}\dfrac{\partial A}{\partial n} = -H_t \end{cases} \quad (3)$$

where $S1$ is the first boundary condition, $S2$ is the second boundary condition. These boundary conditions are equivalent to the conditional variational problem of energy function.

$$\begin{cases} W(A) = \iint\limits_{\Omega}\left(\int_0^B \frac{1}{\mu_r \mu_0} B dB - J_z A\right) dxdy - \int\limits_{S_2}(-H_t) A dl = \min \\ A = A_0 \end{cases} \quad (4)$$

where $B = \sqrt{\left(\frac{\partial A}{\partial x}\right)^2 + \left(\frac{\partial A}{\partial y}\right)^2}$.

The solution of regional Ω can be discredited into a series of units. By using corresponding unit interpolation displacement function, the above function can be calculated by the following:

$$[K]_\Omega [A_z]_\Omega = [P]_\Omega \quad (5)$$

where $[K]_\Omega$ is the element coefficient matrix, $[P]_\Omega$ is the margin vector. And the problem of electromagnetic field PMSLM has been converted to pure mathematics problems. It can be solved by using Newton Raphson iterative method.

III. Analysis of Thrust and Magnetic flux

A. The Reason and Minimization of Force Ripple.

The detent force is composed of cogging force and end force. By choosing appropriate boundary conditions, the end effect of unit motor model can be ignored. So, the cogging is the main part of the detent force. Essentially, the creation of cogging force is due to the primary slot. The interactions between permanent magnet poles and the primary pole and slot have changed the air gap permeance between secondary and primary, the magnetic resistance and energy storage of magnetic field have changed with the position of motion, and these changes create thrust ripple. When the motion moves a tooth pitch the change occurred periodically, and has no correlation with the armature current.

The detent force plays an important role in the thrust ripple in PMLSMs. And these force pulsations contribute to vibrations and acoustic noise of PMLSMs. Especially at low speed operation, the ripple can cause resonance, which affects operation performances of the system. So the effect must be reduced in driving system. There are many approaches to improve the detent force profile. One approach is to choose suitable control strategy. Another approach is to modify the structure of motor. This research makes an attempt to improve the force profile by the geometry modifications approach which is to provide pole shoes on the primary poles.

Generally, the percentage thrust ripple is defined as:

$$Force \quad Ripple = \frac{F_{\max} - F_{\min}}{F_{avg}} \times 100\% \quad (6)$$

where $F_{\max}$ is the maximum value of the force, $F_{\min}$ is the minimum value of force and F_{avg} is the value of average force.

B. Analysis of Primary Pole Width

This research aims at determine the improvement in the force profile when the primary pole width gets varied. The motor uses fraction slot structure to reduce the thrust ripple. The difference between integral slot and fractional slot has been researched in reference [8]. The shape of original PMLSM is shown in Fig. 1. And the specifications of it are given in Table I.

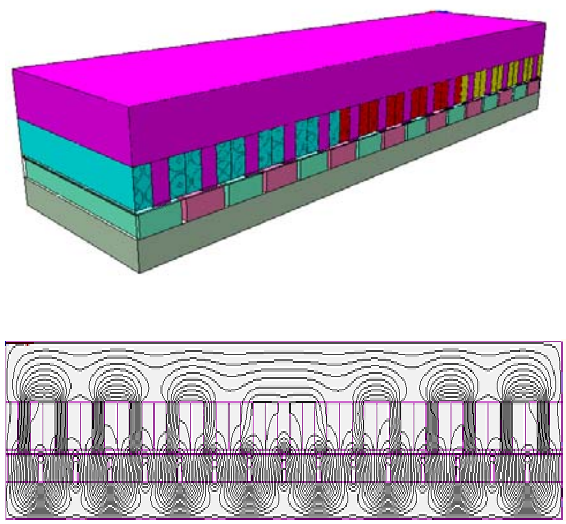

Figure 1. 3D view and flux lines of the original PMLSM.

TABLE I.
SPECIFICATIONS AND DIMENSIONS OF PMLSM.

Name and Unit	Value
width of the primary pole [mm]	7
width of the primary slot [mm]	18
primary pole height [mm]	20
air gap length [mm]	1
width of permanent magnet [mm]	20
permanent magnet height [mm]	11
number of turns per phase	200

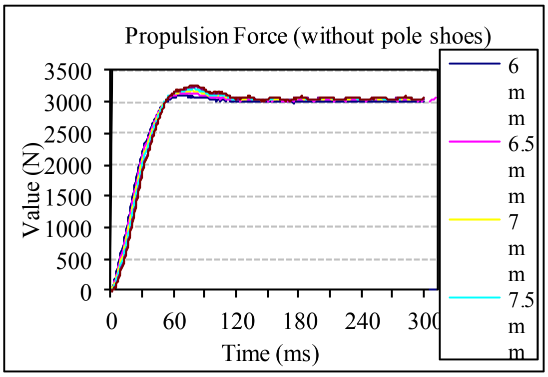

(a) Propulsion force with various pole width.

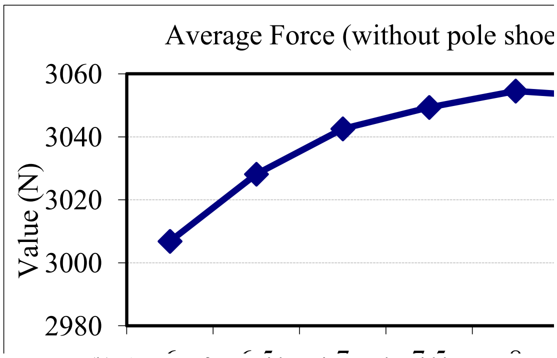

(b) Average force with various pole width.

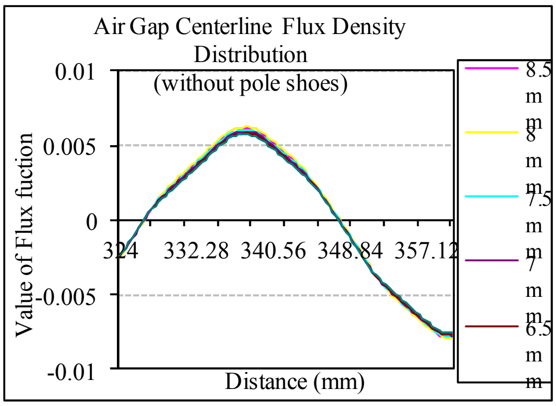

(c) Air gap centerline flux density distribution.

Figure 2. Force and Flux for various primary pole widths (without pole shoes).

The width of the primary pole (W_{P1}) is varied from 6 mm to 8.5 mm in steps. The propulsion force, average force and magnetic flux profiles are shown in Fig. 2. The secondary remains unchanged throughout the research. The height of the primary pole is fixed. The field analysis has been carried out for three phase sinusoidal excitation of 90 V. From Fig. 2(b), it can be observed that, when the primary pole width is increased from 6 mm to 8 mm, there is an increase in the average force. And there is a maximum average force (F_{avg}) occurring when the pole width changes.

From Fig. 2(c), it can be observed that the value of magnetic flux is maximized when the pole width is 8 mm. As the width decreasing, decreasing width will lead to the magnetic saturation. The magnetic flux density becomes small with the width over 8 mm.

TABLE II.
COMPARISON OF FORCE FOR VARIOUS PRIMARY POLE WIDTHS (WITHOUT POLE SHOES)

W_{P1} [mm]	$F_{\max}$ [N]	$F_{\min}$ [N]	F_{avg} [N]
6	3020.933	2987.631	3006.811
6.5	3045.807	3007.068	3028.148
7	3064.335	3020.607	3042.54
7.5	3076.024	3021.872	3049.338
8	3083.114	3025.903	3054.531
8.5	3086.101	3015.476	3052.776

Table II summarizes the comparison of the studied configurations and shows the primary pole width vs. average force. With the increasing of pole width from 6 mm to 8 mm, the average force has a 1.587% increase. It is generally accepted that decreasing the primary pole width will decrease the aligned inductance with negligible effect on the unaligned inductance. But from Table II, when the width of primary pole is more than 8 mm, the average force is lower than 8 mm.

C. Analysis of Thrust Ripple Minimization

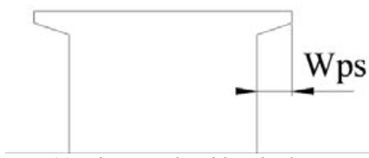

(a) Primary pole with pole shoe.

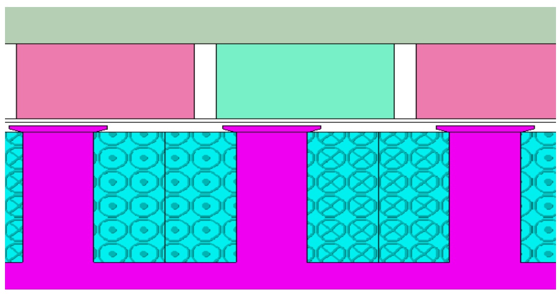

(b) Optimized motor with primary pole shoes.

Figure. 3. Geometry of pole shoes and optimized motor.

In this section, the improvement of thrust force profile by using primary pole shoes is investigated by 2-D finite-element analysis. The width of the primary pole shoe (W_{PS}) is varied from 0 mm to 2 mm in steps. The differences between original and optimized pole shape are shown in Fig. 3.

The aim of proposing the primary pole shoe is to widen the primary pole width to smoothen the force profile. The width of the pole and overall height of the primary pole are maintained constant. The simulation is presented for a three phase sinusoidal excitation of 90 V. The propulsion force, magnetic flux profiles and the rate of thrust ripple when the pole shoe width is increased from 0 mm to 2 mm are shown in Fig. 4.

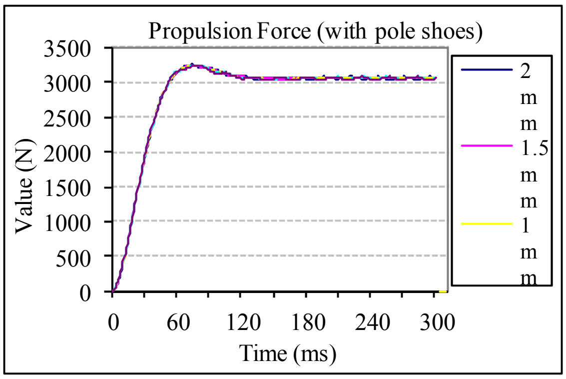

(a) Propulsion force with various pole shoes width.

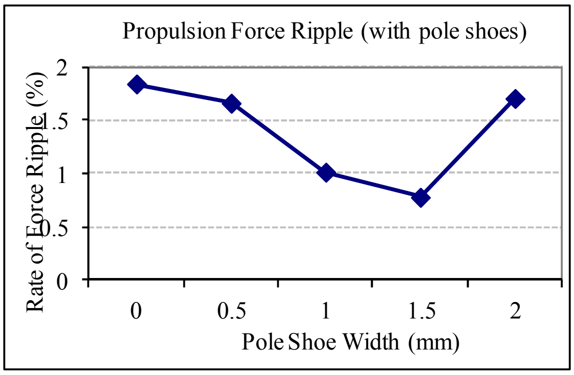

(b) Propulsion force with various pole shoes width.

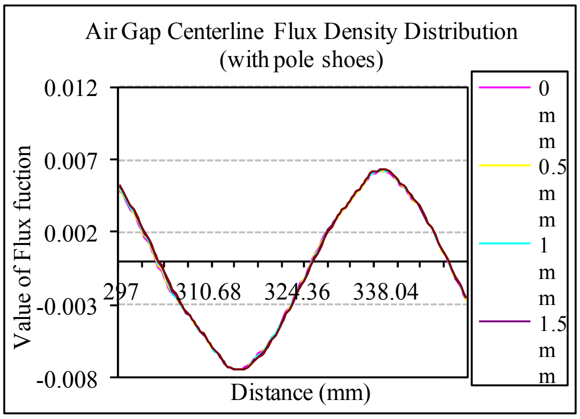

(c) Air gap centerline flux density distribution (with pole shoes).

Figure. 4. Force for various primary pole shoe widths (with pole shoes)

Fig. 4(b) shows thrust ripple with the primary pole shoes width. From Fig. 4(b), the low thrust ripple occurs when the primary pole shoe width is 1.5 mm. When the pole shoe width increases from 0 mm to 1.5 mm, the force ripple keeps decreasing. But, when the width of pole shoe is more than 2 mm, a big fluctuation will be caused.

TABLE III.
COMPARISON OF FORCE FOR VARIOUS PRIMARY POLE SHOE WIDTHS (WITH POLE SHOES).

W_{PS} [mm]	$F_{\max}$ [N]	$F_{\min}$ [N]	*Rate of Force Ripple* [%]
0	3083.114	3025.903	1.843607
0.5	3084.91	3034.067	1.662693
1	3078.441	3047.393	1.014306
1.5	3072.293	3048.455	0.778488
2	3082.523	3030.232	1.707289

Table III summarizes the comparison of studied configurations with different pole shoes. From Table III the provision of primary pole shoes improves the force profile and reduces the thrust ripple. With the increasing of shoe width from 0 mm to 1.5 mm, the thrust ripple has been decreased by 57%.

From Fig.4(c), the extent of the high magnetic flux region along the centerline of air gap is increased by using pole shoes. As the width of pole shoe is increased, keeping the width of pole as constant, the value of flux is increased, and the rate of thrust ripple keeps a decrease until the width of pole shoe up to 1.5 mm.

Comparing Table II with Table III, keeping the primary pole shoe width as constant, there is a maximum average force as a suitable pole width. And these tables also depicts that keeping the width of pole as constant, there is a minimum thrust ripple occurring in a suitable pole shoe width.

Finally, from the 2-D FEA field simulation, the optimized PMLSM has less thrust ripple when compared with the original motor. The rate of detent thrust ripple reduces from 0.5626% to 0.2134%.

IV. MORE SIMULATION AND MOTOR PERFORMANCE

A. Performance with Various Load

Cause of the self-starting performance of synchronous motor is carried out by means of special structure or special control circuit. During the simulation, the speed motion is given at 0.3 m/s. When the speed increases to a new stable state, a step load is given. The amplitudes of fundamental armature current with load variations are derived by the Fourier decomposition and shown in Fig. 5.

The efficiency μ and power factor $\cos\varphi$ can be calculated as follows:

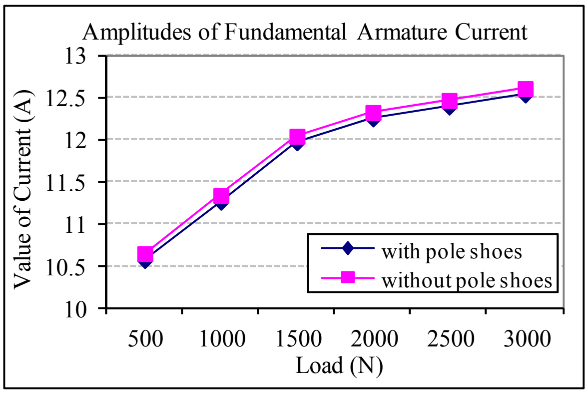

Figure 5. The amplitudes of fundamental armature current with laod variations.

$$\eta = \frac{Fv_s}{Fv_s + 3I_s^2 r_s} \tag{7}$$

$$\cos\varphi = \frac{Fv_s + mI_s^2 r_s}{3U_s I_s} \tag{8}$$

where F is average thrust, I_s and U_s is the effective value of armature current and voltage, r_s is armature resistance, and v_s is the velocity of synchronous speed.

The influences of load variation on efficiency and power factor are shown in Fig. 6.

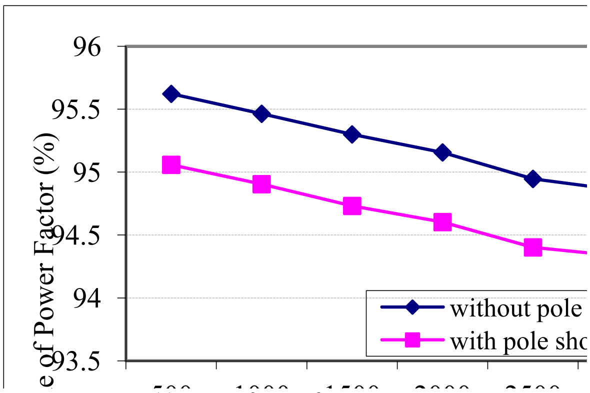

(a) Power factor of motor cosφ.

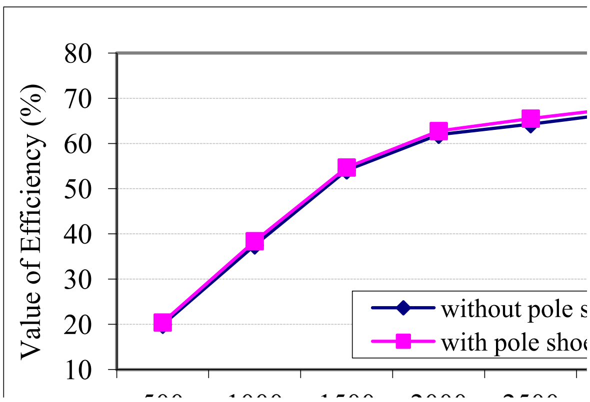

(b) Efficiency of motor μ.

Figure. 6. Power factor and efficiency with different load.

The comparisons of power factor and efficiency between optimized motor and original motor are shown in Fig. 6. The power factor and efficiency are improved by affixing pole shoes. With the load increasing, the efficiency and power factor are rising.

In practice, there is an influence of step load on velocity. Fig.7 shows that the motor with pole shoes has faster reaction rate and better motion following ability.

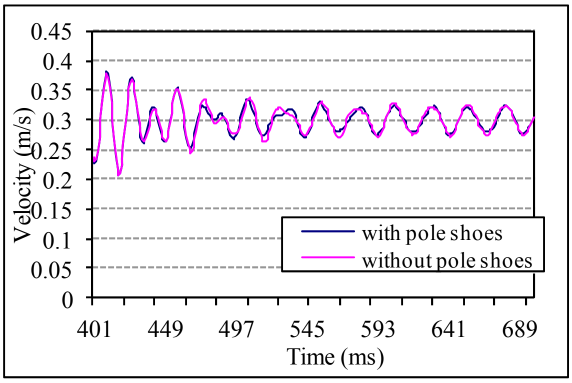

Figure. 7 The influence of step load on velocity.

B. Back EMF of PMLSM

The PMLSM is simulated at 0.3 m/s velocity and with no-load. The back EMF of the optimized PMLSM is shown in Fig. 8.

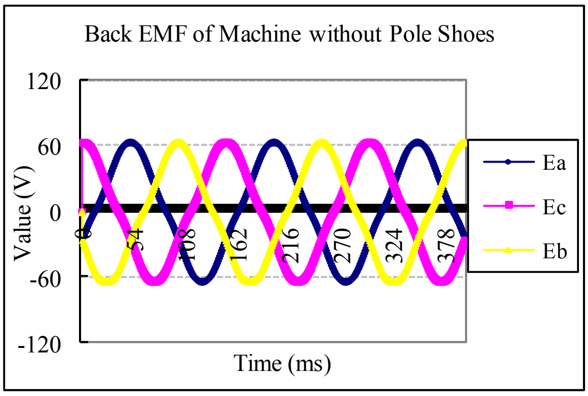

(a) Back EMF of original PMLSM.

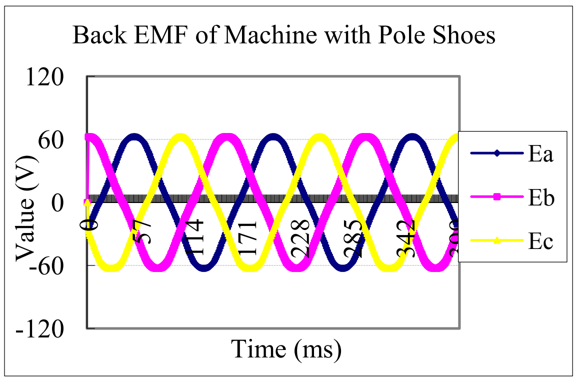

(b) Back EMF of optimized PMLSM.

Figure. 8. The back EMF of motor.

As fig.8 shown, the EMF of three phases, E_a, E_b, E_c have the same amplitude. The v is the velocity of primary, the back EMF constant of original motor is calculated as follows:

$$K_{e1} = \frac{E_{a1}}{v} = \frac{45.05}{0.3} = 150.17 \quad \text{Vp - nrms/m/s} \quad (9)$$

The back EMF constant of optimized motor is:

$$K_{e2} = \frac{E_{a2}}{v} = \frac{44.29}{0.3} = 147.64 \quad \text{Vp - nrms/m/s} \quad (10)$$

From (4), (5) and Fig. 8 it can be observed that, the change of the back EMF of the optimized motor is limited. So there is not an obvious decrease in the propulsion force. The new geometry of motor does not affect the control performance. And the decrease is also good for the starting performance.

V. CONCLUSION

Two dimensional finite element analyses of permanent magnet linear synchronous motor with new primary pole geometry have been carried out. There is a maximum magnetic flux density and thrust force while the pole width increases to a certain value. With pole shoes, the thrust ripple of PMLSM can be reduced obviously. The changes of thrust force were confirmed by increases of magnetic flux density. The efficiency and power factor of optimized motor with different load are higher than original one. The change of back EMF constant is limited. So the motor can keep a good starting performance. And all of these will contribute to PMLSM optimization.

ACKNOWLEDGMENT

This work was supported by the National Natural Science Foundation of China (NO.61074095), and Henan Outstanding Person Plan (NO. 104200510021), and Ministry of Education Scientific Research Foundation for Chinese Overseas Returnees and Ministry of Education Research Fund for Doctoral Program of Higher Education, and Henan Province Key Project (NO. 092102210359) and Doctoral Fund of Henan Polytechnic University.

REFERENCE

[1] Wang Xu-dong, Yuan Shi-ying, Jiao Liu-cheng, Wang Fu-zhong, Wang Zhao-an. Principle and Present Study Situation of Permanent Magnet Linear Synchronous Motor for Vertical Transportation System. Micromotors Servo Technique [J]. 2000.05: 35-38

[2] Li Qing-lei, Wang Xian-kui, Wu Dan, Liu Cheng-ying, Shi Zhong-dong. Thrust fluctuation analysis and reduction of PMLSM. JOURNAL OF TSINGHUA UNIVERSITY (SCIENCE AND TECHNOLOGY) [J]. 2000.05: 33-36

[3] Xu Yue-tong, Fu Jian-zhong, Chen Zi-chen. Thrust Ripple Optimization and Experiment for PMLSM. Proceedings of the Csee[J]. 2005.12: 122-126

[4] Xia Jia-kuan, Yu Bing. Influence of Stator Teeth Notching on the Cogging Torque of Permanent Magnet Motor. Micromotors [J]. 2010.07:13-16

[5] Chen Xia, Zou Ji-bin, Hu Jian-hui. Reducing the Cogging Torque of PM Motor by Stator Teeth Notching. Small & Special Electrical Motors [J]. 2006.11: 9-10,42

[6] Wang Xu-dong, Feng Hai-chao, Xu Xiao-zhuo, Si Ji-kai, ShangGuan Xuan-feng, Yuan Shi-ying. The review of research on detent force of Permanent magnet motor (I) - The cogging torque of rotating permanent magnet motor. The 2008 national academic annual meeting of linear motor, modern drive and system. 2008.09: 6-13

[7] Wang Xu-dong, Feng Hai-chao, Xu Xiao-zhuo, Si Ji-kai, ShangGuan Xuan-feng, Yuan Shi-ying. The review of research on detent force of Permanent magnet motor (Ⅱ) - The detent force of permanent magnet linear motor. The 2008 national academic annual meeting of linear motor, modern drive and system. 2008.09: 14-18

[8] ShangGuan Xuan-feng, Feng Hai-chao. The characteristic analysis and comparison of Integer slot and fractional slot PMLSM. The 2010 national academic annual meeting of linear motor, modern drive and system. 2010.10:113-117

[9] Feng Hai-chao, Wang Xu-dong, Xu Xiao-zhuo. The characteristic analysis and experimental of PMLSM for Vertical elevator. The 2010 national academic annual meeting of linear motor, modern drive and system. 2010.10:106-112

[10] N.C.LENIN, R.ARUMUGAM, V.CHADRESEKAR. Force Profiles of a Linear Switched Reluctance Motor Having Special Pole Face Shapes. Advances in Electrical and Computer Engineering [J]. 2010.04:129-134

[11] Du Wei-min, Wang Xu-dong, Xu Xiao-zhuo, Feng Hai-chao. Research on Minimizing Detent Force of Linear Permanent Magnet Brushless DC Motor. Small & Special Electrical Motors [J]. 2008.11: 9-14

[12] Wang Xu-qiang, Wang Xu-dong, Du Wei-min, Yu Lin. Research on minimizing Detent Force of Permanent Magnet Linear Synchronous Motor. Micromotors [J]. 2009.12: 28-30,46

[13] Yue-tong Xu, Jian-zhong Fu, Zi-chen Chen. Thrust ripple optimization and experiment for a permanent magnet linear synchronous motor. Frontiers of Electrical and Electronic Engineering in China. 2005.12: 122-126

[14] In-Soung Jung, Jin Hur, Dong-Seok Hyum. 3-D analysis of permanent magnet linear synchronous motor with magnet arrangement using equivalent magnetic circuit network method. IEEE Transactions on Magnetics 1999, 35(5): 3736-3738

[15] Mi-Yong Kim, Yong-Chul Kim, Gyu-Tak Kim. Design of Slotless-Type PMLSM for High Power Density Using Divided PM. IEEE Transactions on Magnetetics, 40(2): 746-749

[16] Carl G. Jeans, Rupert J. Cruise, Charles F. Landy. Methods of Detent Force Reduction in Linear Synchronous Motors. IEEE African Conference, 1999, (2): 437-439

[17] In-Soung Jung, Sang-Baeek Yoon. Analysis of force in a short primary type and a short secondary type permanent magnet linear synchronous motor. IEEE Transactions on Energy Conversion, 1999, 14(4): 1265-1270

[18] Akio Yamamoto, Toshiki Niino, Toshiiro Higuchi. Modeling and identification of an electrostatic motor. Precision Enginering, Vol.30, No.1, pp104-113, January, 2006

[19] H. Arof, A. M. Eid and K. M. Nor. Cogging force reduction using special magnet design for tubular permanent magnet linear generators. Proceedings on 39th International Universities Power Engineering Conference (UPEC), 2004, (2): 523-527

Xudong Wang was born in China in 1967, and received the PH.D degree in electrical engineering from School of Electrical engineering, Xi'an Jiaotong University, China, in 2002. From 2003 to 2004, he was carried out the postdoctoral research project in the University of Sheffield, UK, as a visiting scholar. His research interests are linear motor theory and application, motor optimization, design of linear motor driving system, energy efficient motors.

He is a professor and director of Institute of Linear Electric Machines & Drives (LEMD) in Henan Polytechnic University. he accomplished 25 research projects, including 4 the National Natural Science Foundation of China, and over 80 papers was published. He made 13 national invention patents and 9 utility model authorization patents. He presided to develop many experimental system or products, such as rope-less hoist system with high-power, home elevator driven by PMLSM, automatic precision servo system, high temperatures superconducting Maglev vehicles, efficient asynchronous motor, self-starting PM motor, and so on. Now, He is dedicated to the research concentrated mostly on multi-car rope-less hoist system driven by PMLSM and efficient motor,etc.

Dr. Wang is the one of the academic technology leaders, key academic leader of key discipline of Motor and Electrical, Science and Technology Innovation outstanding talent in Henan Province, China. He is the member of the International Electromagnetic (ICS) and linear motor committee of China.

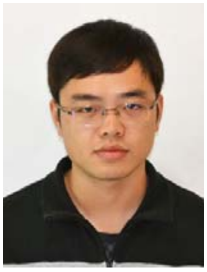

Kai Cao was born in China in 1985, and received the B.S. degree in automation from School of Computer and Information Engineering, Henan University, china, in 2008. From 2009 to 2011, he study for M.S. degree in control theory and control engineering from School of Electrical Engineering and Automation, Henan Polytechnic University, china.

His research interests are the optimization design of linear and rotary machines, the simulation and analysis of special motor.

Mr. Cao is studying in institute of linear electric machine and drives, Henan Province, China. In recent years, he takes part in some provincial or country research projects, published 2 academic papers.

Haichao Feng was born in China in 1983, and received the B.S. and M.S. degrees in electrical engineering and automation, control theory and control engineering from School of Electrical Engineering and Automation, Henan Polytechnic University, china, in 2005 and 2008, respectively. His research interests are the optimization design of linear and rotary machines, power electronics, and their controls.

From 2007 to 2008, he was with ASM Pacific Technology Ltd., HongKong, as a Research Engineer. New, he is a teacher in School of Electrical Engineering and Automation, Henan Polytechnic University, china.

Mr. Feng is a member of institute of linear electric machine and drives, Henan Province, China. In recent years, he participates in 5 provincial and 2 country research projects, published more than 8 academic papers.

Lili Guo was born in China in 1986, and received the B.S. degree in electrical engineering and automation from Henan Polytechnic University, china, in 2009. From 2009 to 2011, she study for M.S. degree in electrical power system and automation from School of Electrical Engineering and Automation, Henan Polytechnic University, china.

Her research interests are the analysis and design of electrical, the research of smart power grid. In recent years, she takes part in some provincial or country research projects, published some academic papers.

Ms. Guo is studying in electrical power system and automation from School of Electrical Engineering and Automation, Henan Polytechnic University, china. In recent years, she takes part in some provincial or country research projects, published 2 academic papers.

Xiaozhuao Xu was born in China in 1980, and received the B.S. and M.S. degrees in electrical engineering and automation, motor and electrical from School of Electrical Engineering and Automation, Henan Polytechnic University, china, in 2003 and 2006, respectively. His research interests are the analysis of physical field for special motor, optimization design of linear and rotary machines.

From 2007 to 2008, he was with ASM Pacific Technology Ltd., HongKong, as a Research Engineer. New, he is a teacher in School of Electrical Engineering and Automation, Henan Polytechnic University, china.

Mr. Xu is a member of institute of linear electric machine and drives, Henan Province, China. In recent years, he participates in 8 provincial and 2 country research projects, published more than 10 academic papers.